JOURNAL OF GEOPHYSICAL RESEARCH, VOL. 101, NO. C5, PAGES 12,177–12,191, MAY 15, 1996

Modeling the diurnal cycle of carbon monoxide: Sensitivity to physics, chemistry, biology, and optics

Anand Gnanadesikan[1]

Department of Physical Oceanography, Woods Hole Oceanographic Institution, Woods Hole, Massachusetts

Abstract. As carbon monoxide within the oceanic surface layer is produced by solar radiation, diluted by mixing, consumed by biota, and outgassed to the atmosphere, it exhibits a diurnal cycle. The effect of dilution and mixing on this cycle is examined using a simple model for production and consumption coupled to three different mixed layer models. The magnitude and timing of the peak concentration, the magnitude of the average concentration, and the air-sea flux are considered. The models are run through a range of heating and wind stress and compared to experimental data reported by *Kettle* [1994]. The key to the dynamics is the relative size of four length scales; D_{mix}, the depth to which mixing occurs over the consumption time; L, the length scale over which production occurs; L_{out}, the depth to which the mixed layer is ventilated over the consumption time; and L_{comp}, the depth to which the diurnal production can maintain a concentration in equilibrium with the atmosphere. If $D_{mix} \gg L$, the actual model parameterization can be important. If the mixed layer is maintained by turbulent diffusion, D_{mix} can be substantially less than the mixed layer depth. If the mixed layer is parameterized as a homogeneous slab, D_{mix} is equivalent to the mixed layer depth. If $D_{mix} > L_{out}$, production is balanced by consumption rather than outgassing. The ratio between D_{mix} and L_{comp} determines whether the ocean is a source or a sink for CO. The main thermocline depth H sets an upper limit for D_{mix} and hence D_{mix}/L, D_{mix}/L_{out}, and D_{mix}/L_{comp}. The models are run to simulate a single day of observations. The mixing parameterization is shown to be very important, with a model which mixes using small-scale diffusion producing markedly larger surface concentrations than models which homogenize the mixed layer completely and instantaneously.

1. Introduction

A number of important chemical species (oxygen, carbonyl sulfide, carbon monoxide, hydrogen peroxide) are known to exhibit diurnal variability in the upper ocean. For a given trace species, the amplitude and timing of this daily cycle can be affected by a number of different processes including (1) how quickly and where it is produced; this is determined by the optics and local water chemistry (for carbon monoxide, carbonyl sulfide, and hydrogen peroxide) or biology (for oxygen), (2) the rate at which it is consumed which can be determined in turn by water temperature, local biology, or chemistry, (3) the rate at which it is transferred between the atmosphere and ocean, and (4) the rate at which it is mixed into the water column.

If the balance between consumption and production is local (there is no mixing or gas exchange), the diurnal cycle is reasonably simple to understand. The important constants are just the consumption rate and production constants. Since they determine where the sunlight is absorbed, the optical properties of the water are very important. If the consumption rate is much larger than 1 d^{-1}, the concentration follows the solar forcing. If it is $O(1\ d^{-1})$ or smaller, the maximum concentrations are seen at the end of the day.

In the presence of mixing, however, the picture becomes more complicated. The importance of the optical properties of the water, the timing of the maximum concentration, and the partition between gas exchange and consumption as sink terms can all depend on the mixing. This paper uses the diurnal cycle of carbon monoxide (CO) in order to attack the following four questions:

1. When is dilution important in determining the surface concentration and flux of a photochemically produced trace species such as CO?
2. How sensitive is the diurnal cycle to the exact parameterization of the optics, consumption, and outgassing, and how does such sensitivity depend on the mixing?
3. How sensitive are the results to different parameterizations of the dilution? One question of particular interest is the difference between slab models, which homogenize the mixed layer instantaneously and completely, and eddy viscosity models which require some time for the mixed layer to become homogenized.
4. When can a tracer such as CO be used to improve understanding of the physics governing mixing in the upper ocean?

This paper approaches the problem as follows. A simple model of the photochemical production and biological consumption based on observations of *Kettle* [1994] and A. J. Kettle et al. (manuscript in preparation, 1996, hereinafter referred to as KEA) is developed in section 2. This simple model

[1]Now at Program in Atmospheric and Oceanic Sciences, Princeton University, Princeton, New Jersey.

Paper number 96JC00463.
0148-0227/96/96JC-00463$09.00

is coupled to three operational mixed layer models briefly described in section 2.2. Within this model framework, five key length scales are then identified. These are D_{mix}, the depth to which mixing occurs over the consumption time of the trace species (as will be shown, D_{mix} can depend critically on the mixing parameterization); L, the length scale over which production occurs; L_{out}, the depth to which the mixed layer is ventilated over the consumption time of the trace species; L_{comp}, the depth to which the diurnal production can maintain a concentration in equilibrium with the atmosphere, and H, the depth of the permanent stratification. Section 3 shows how the relative sizes of these length scales determine which processes are important.

In section 4 the models are used to simulate the diurnal cycle under a range of forcing conditions and to simulate a particular day's observations, thus exploring which dynamical regimes are important for CO in an open ocean environment. The particular day chosen lies within a regime where not only dilution but also its parameterization is extremely important in setting the diurnal cycle. In particular, a model in which CO diffuses slowly through the mixed layer is shown to trap CO near the surface in comparison to slab models which mix the layer completely at each time step. This paper complements recent work by *Sikorski and Zika* [1993a, b] on hydrogen peroxide, *Kettle* [1994], KEA, and *Doney et al.* [1995] on carbon monoxide, and *McNeil and Farmer* [1995] on oxygen. In particular, it extends their work by examining the interdependence of mixing, photochemistry, outgassing, and biological consumption, by indicating the sensitivity of particular results to each process, and by providing a conceptual framework within which their results can be evaluated.

2. Background and Models

2.1. Carbon Monoxide: General Background

It has long been realized that CO exhibits strong diel variability in the upper ocean. *Swinnerton et al.* [1970] showed that the concentration of carbon monoxide (CO) off of Barbados varied by as much as a factor of 10 over the course of a day, reaching concentrations as high as 100 nL/L. *Conrad et al.* [1982], *Conrad and Seiler* [1986], *Jones* [1990], *Kettle* [1994], and KEA extended these observations, showing that such cycles could be found over much of the Atlantic. Figure 1a is taken from *Kettle* [1994] and shows the concentration of CO as a function of depth at several times during the day. The data shown are from the subtropical Atlantic. Large concentrations, of order 1.5 nM, are seen during the day, with return to values of 0.5 nM at night. Figures 1b–1d show subsurface profiles of CO concentration. Note that in all three profiles a subsurface maximum is seen. Nonetheless, the profile of CO concentration is more uniform than might be assumed from a simple local balance between production by solar radiation and consumption by biota which would tend to result in an exponential distribution.

CO is produced by photochemical reactions, probably involving dissolved organic compounds [*Conrad and Seiler*, 1980, 1982; *Mopper et al.*, 1991]. The production is primarily driven by light in the blue end of the spectrum [*Kettle*, 1994; KEA]. A simple parameterization may be obtained by defining Q_0 as the shortwave radiative flux at the ocean surface and letting P_{con} be the concentration of CO produced in 1 hour by the deposition of 1 W of sunlight in a cubic meter of water, and L as the e-folding scale of the light responsible for the production. Then $P(z, t)$, the production in nanomoles per hour is given by

$$P(z, t) = P_{con} Q_0(t)/L \; e^{z/L} \tag{1}$$

In reality, the production will have a much more complicated variation, since both P_{con} and L will be functions of the wavelength of the radiation. *Sikorski and Zika* [1993a] presented such a model for H_2O_2 and a similar task has been undertaken for carbon monoxide [*Kettle*, 1994; KEA]. The complicated optics involved in such models are neglected here so as to bring out the principal dependence on penetration depth.

A range of L is considered which are reasonable for CO. From KEA, an average e-folding depth of 8 m and P_{con} of 14 nmol $(W/m^2)^{-1}$ h^{-1} is estimated for the day shown in Figure 1a. This study looks at three values of L: 23 m, 8 m, and 2 m. P_{con} (which yields a fairly low value for surface production compared to the results of *Jones and Amador* [1993] and is slightly lower than the surface values estimated by *Mopper et al.* [1991] in the Sargasso Sea) is, in general, a function of water type and so might be expected to be related to L. Such relationships are neglected in the current paper, so that the separate effects of varying P_{con} and L may be considered. When all the CO is broken down within the water column, all concentrations predicted are proportional to P_{con}. When gas exchange (both invasion and evasion) is important, the picture is more complicated, a fact which should be kept in mind when applying these results to other waters.

Biological consumption is thought to play a critical role for CO. In dark incubation experiments, CO concentration drops over time. The consumption is shut off when the water is poisoned or when it is filtered. This has led a number of investigators to propose that bacteria are the primary consumers of CO [*Conrad and Seiler*, 1982; *Conrad et al.*, 1982; *Jones and Morita*, 1983], turning it into CO_2. This work models the consumption as being proportional to the concentration with a rate constant $1/T_{con}$. Letting $C(z, t)$ be the consumption of the trace species and $[CO](z, t)$ be the concentration, the equation for consumption is

$$C(z, t) = -[CO](z, t)/T_{con} \tag{2}$$

In the absence of mixing and outgassing, the timing of the maximum in CO concentration is a strong function of T_{con}. When T_{con} is very large, the concentration reaches its peak at the end of the day, whereas when T_{con} is very small, the concentration simply tracks the production. Published values for T_{con} seem to vary greatly from location to location and season to season. *Jones and Amador* [1993], for example, report T_{con} as low as 2 hours and as high as 108 hours in the Orinoco River plume, with a range of 8–70 hours in the central Caribbean. For the observations in Figure 1a, *Kettle* [1994] reported consumption times between 24 and 100 hours. This work uses four values of T_{con}, 6 hours (allowing for almost all of the production to be consumed overnight), 12 hours, 20 hours (a value more in line with *Conrad and Seiler* [1982] and consistent with one of the incubations of *Kettle* [1994]), and 52 hours (a value reported by *Kettle* [1994] which allows for production to be carried over to following days).

Observations show that the peak value of CO concentration depends on wind stress. Figure 2 is taken from *Conrad et al.* [1982] and shows the dependence of the surface CO concentration, normalized for insolation, versus wind speed. At high wind speeds the "yield" of CO is sharply reduced, and the

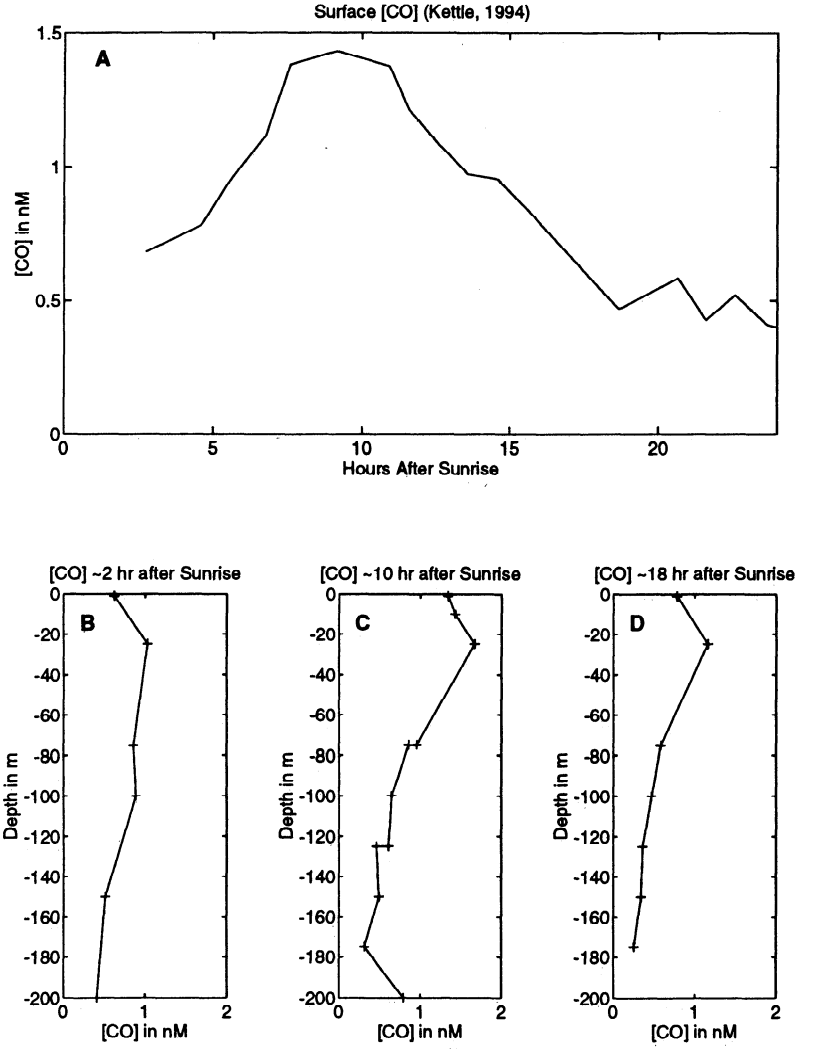

Figure 1. Observations of diurnal cycling of carbon monoxide in the open ocean. Data are from *Kettle* [1994] and KEA and are presented courtesy of the authors. (a) CO concentration at the surface in n*M* as a function of time in hours after sunrise. (b) CO concentration at various depths approximately 1 hour after sunrise. (c) CO concentration at various depths approximately 8 hours after sunrise. (d) CO concentration at various depths approximately 18 hours after sunrise.

concentration asymptotes toward being in balance with the atmosphere. (It should be noted, however, that *Kettle* [1994] does not see such a clear signal. On the day shown in Figure 1, the mean wind speed is close to 13 m/s, yet there is still a strong diurnal signal.) There are two possible explanations for this, enhanced mixing and outgassing to the atmosphere. Because the upper ocean is highly supersaturated with respect to the atmosphere, the oceans are a net source of CO. This may have some geochemical importance. *Mopper et al.* [1991] presented evidence that the photochemical process producing CO is the major pathway by which dissolved organic carbon (DOC) is broken down. As will be shown in this paper, the diurnal cycle of mixing plays an important role in determining how much of the resulting CO is outgassed to the atmosphere and how much is consumed by biology. The outgassing term is treated first (the mixing term will be covered in the following section 2.2).

The air-sea exchange of CO is given by the formula of *Liss and Merlivat* [1986] using a Schmidt number of 608.7. Defining F_{CO} as the CO flux:

$$F_{CO} = k_w\{[CO](z = 0, t) - [CO]_{eq}(p, T)\} \quad (3a)$$

$$k_w = 4.68 \times 10^{-7}u \quad u < 3.6 \quad (3b)$$

$$k_w = 7.81 \times 10^{-6}u - 2.66 \times 10^{-5} \quad 3.6 < u < 13 \quad (3c)$$

$$k_w = 1.63 \times 10^{-5}u - 1.36 \times 10^{-4} \quad u > 13 \quad (3d)$$

where k_w is the piston velocity in m s^{-1}, $[CO]_{eq}(p, T)$ is the concentration for which the trace species is in equilibrium with the atmosphere as a function of pressure and temperature, and u is the wind speed in m s^{-1} at a reference height of 10 m. The Liss-Merlivat model was shown to work in high wind speeds by *Watson et al.* [1991]. For a wind speed of 5 m s^{-1}, the piston velocity is 1.25×10^{-5} m s^{-1}, so that over the course of a day, a mixed layer 1 m or so in thickness would be ventilated by the atmosphere. If the wind speed is 20 m s^{-1} the piston velocity is 1.9×10^{-4} m s^{-1}, so that over the course of a day, a mixed layer 16 m thick would be ventilated. (The approach taken here is somewhat different from that of *Conrad et al.* [1982] and

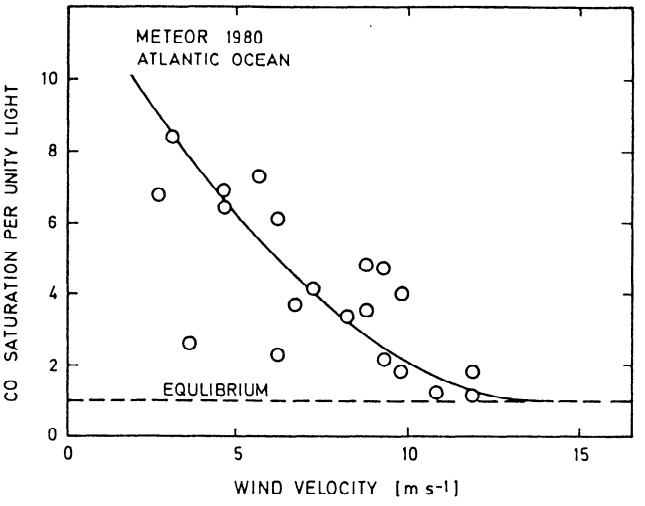

Figure 2. Daily average CO saturation normalized to a daily average light intensity of 100 W/m^2 as a function of the daily average wind speed observed at a height of 20 m. Figure taken from *Conrad et al.* [1982] representing data taken from the *Meteor* 1979 cruise.

Conrad and Seiler [1986], who assume a mean transfer velocity of about 8 m d^{-1} corresponding to a mean wind speed of about 10 m s^{-1}. This paper considers the fact that such a mean wind speed will also produce increased mixing and thus increased dilution. As noted by *Wanninkhof* [1992], because the gas transfer velocity is highly nonlinear, the gas transfer velocity predicted by (3) using an average wind speed will underestimate the true average gas transfer velocity.) If there is significant chemical interaction within bubbles or slicks, the Liss-Merlivat formula will underestimate the rate of gas transfer. This possibility is considered in more detail in section 4.

To summarize then, the baseline values of constants are a production constants P_{con} of 14 nmol W^{-1} h^{-1}, an e-folding scale L for the production of 8 m, a consumption time T_{con} of 52 hours, and outgassing given by the Liss-Merlivat formulation with $[CO]_{eq}$ = 0.5 nM. This baseline set of chemical constants is based on the work of *Kettle* [1994] as modified by KEA and will be referred to throughout as the KEA constant set. Whenever different values of the P_{con}, T_{con}, L, or outgassing are used, they are specifically noted.

2.2. Physical Mixing Models

The photochemical model is coupled to a total of three mixing models. All these models behave in broadly similar ways. When the wind is weak and the insolation is strong, the upper ocean becomes stratified and a shear layer develops. When the wind is strong and the insolation is weak, mixing penetrates into the water column. In the presence of evaporation or heat loss at the surface, all three models will overturn. The details of this mixing, however, are different for different models. As a result, the dependence of the mixed layer depth on the wind stress and heat flux is a function of which model is used (recent reviews of these differences are given by *Large et al.* [1994] and *Kantha and Clayson* [1994]).

The first model is a dynamic instability model, presented by *Price et al.* [1986]. In this model the mixed layer is modeled as a slab which is completely and instantaneously mixed. The slab deepens when the shear across the base of the mixed layer becomes too large or when there is heat loss or evaporation at the surface. Below the mixed layer, there is a transition layer, where mixing occurs locally as the result of Kelvin-Helmholu, instability. Kelvin-Helmholtz (K-H) instability arises when the shear dU/dz becomes much larger than the buoyancy, frequency $N = \sqrt{-g/\rho d\rho/dz}$. The effect of K-H instability is to drive the ratio of N to dU/dz toward 1/2. This model, which will be referred to as the PWP model, has become a standard tool for studying mixed layer dynamics. A particular strength is the fact that there are no parameters which need to be tuned to obtain a fit to the case at hand. The PWP model does reasonably well at predicting the diurnal cycle of temperature [*Stramma et al.*, 1986; *Gnanadesikan*, 1994] and has been used to study the observed Ekman spiral under conditions where diurnal restratification is important [*Price et al.*, 1987; *Gnanadesikan*, 1994; *Gnanadesikan and Weller*, 1995]. It is used as an operational model for prediction of sea surface temperature by the U.S. Navy.

The second model is the ocean planetary boundary layer model of *Garwood* [1977], hereinafter referred to as the OPBL model. Like the PWP model, the OPBL model assumes the mixed layer to be a slab. Like the PWP model it uses convective adjustment to homogenize the mixed layer completely when there is surface heat loss. In contrast to the PWP model, however, the slab entrains denser water from below as the result of turbulence generation within the mixed layer (taken to be proportional to the 3/2 power of the wind stress) and as the result of penetrative buoyant convection. The effectiveness of shear-generated turbulence at entraining dense water is reduced as the mixed layer depth increases. The OPBL model is also used as an operational model and has been widely distributed by Naval Postgraduate School. (Although *Garwood* [1977] does allow for entrainment due to shear across the mixed layer base, it is argued that this term is less important than shear-generated turbulence in the mixed layer interior. In subsequent releases of the model, turbulent generation at the mixed layer base is set to zero.)

The third model is a Mellor-Yamada level 2-1/2 level turbulence closure model [*Mellor and Yamada*, 1973, 1982; *Kantha and Clayson*, 1994]. This model computes the eddy diffusivity using the assumption that turbulence is produced by the local stress working against the local shear and by buoyancy transport. The resulting eddy kinetic energy can then be diffused and is lost to turbulent dissipation. The diffusion coefficient K_v is a function of the local turbulent velocity multiplied by a local turbulent length scale. The version of the model used here assumes a constant turbulent length scale throughout the mixed layer. The concentration then evolves according to

$$\frac{d}{dt}[CO] = P(z, t) + C(z, t) + \frac{d}{dz} K_v \frac{d}{dz}[CO]. \quad (4)$$

This model is referred to as the MY2.5 model. For the runs presented here the assumption was made that the turbulent diffusivity for CO was the same as that for temperature. The MY2.5 model is widely used as a mixing model within three-dimensional numerical models of the upper ocean.

All of the mixing in the MY2.5 model occurs as the result of turbulent diffusion. This has three important implications. First, even within the regions in which mixing is strong, there are gradients in the velocity, temperature, and CO concentration. Second, a surface signal in stress, heating, or photochemical production requires time to penetrate to depths near the thermocline. Third, because a surface input of trace gasses or momentum requires some time to come to equilibrium within

a deep mixed layer, processes which act to "consume" such quantities may limit the penetration of the production within the mixed layer. This is not true of the PWP and OPBL models which mix instantaneously and completely.

It should be emphasized at this point that the exact dependence of the mixed layer depth on the wind speedwhen the mixed layer is being heated from above is different in different models. In the OPBL model, for example, the mixed layer depth goes as the minimum of Monin-Obhukhov length

$$D_{\text{mix}} \sim L_{\text{mo}} = \rho c_p u_*^3 / g \alpha Q \tag{5}$$

and the neutral Ekman depth

$$D_{\text{mix}} \sim L_{\text{ek}} = u_* / f \tag{6}$$

where ρ is the density, c_p is the specific heat of water, α is the coefficient of thermal expansion, g is the gravitational constant, u_* is the friction velocity, and f is the Coriolis frequency. In the PWP model, on the other hand, the mixed layer depth goes as [*Price et al.*, 1986]

$$D_{\text{mix}} \sim \sqrt{\rho c_p u_*^4 / T_{\text{insol}} g \alpha Q f^2} = \sqrt{L_{\text{mo}} L_{\text{ek}} / f T_{\text{insol}}} \tag{7}$$

where T_{insol} is the duration of the insolation. Notice that this length scale always depends on the heat flux, while the OPBL model scale does not necessarily.

The models also differ in their response to heat loss or evaporation at the surface. Although both the OPBL and PWP models relieve static instability within the mixed-layer, homogenizing density inversions, the OPBL model allows buoyant convection to entrain water from the thermocline, even when that water is denser than water within the mixed layer. In the PWP model, only shear across the mixed layer base can result in entrainment of denser water, and the MY2.5 model behaves similarly. In general, the OPBL model generates the most mixing, the PWP model somewhat less mixing, and the MY2.5 model the least mixing. There is some limited evidence that the MY2.5 and PWP systematically underpredict the amount of mixing in the upper few meters [*Large et al.*, 1994; *Kantha and Clayson*, 1994].

3. Interactions Between Mixing and Photochemistry: A Typology of Physical Cases

Before plunging into the mechanics of the model runs, it is advisable to develop a framework for considering the role of mixing in the dynamics of a photochemical trace species. The purpose is to present a rough typology of the cases which might be encountered to provide conceptual guidance for interpreting the results of the model runs.

Given a mixed layer with constant depth D_{mix} in which CO concentration is completely uniform, the balance of CO is given by

$$\frac{d}{dt}[\text{CO}] = \frac{P_{\text{con}} Q_0 (1 - e^{-D_{\text{mix}}/L})}{D_{\text{mix}}} - \frac{[\text{CO}]}{T_{\text{con}}} - \frac{k_w([\text{CO}] - [\text{CO}]_{\text{eq}})}{D_{\text{mix}}} + \text{mixing across base} \tag{8}$$

There are at least five length scales which are important in the problem:

1. D_{mix} is the depth to which mixing occurs over the consumption timescale. For a slab model this is just the mixed layer depth. For an eddy viscosity model, however,

$$D_{\text{mix}} \sim \sqrt{K_v T_{\text{con}}} \tag{9}$$

where K_v is the vertical mixing coefficient. The implications of this difference will become clear later in this work.

2. H is the depth of "permanent stratification" or the water depth. It sets an upper limit on D_{mix} over the timescales being considered.

3. L is the e-folding scale for the photochemically active radiation.

4. L_{out} is the outgassing length, which is equal to the piston velocity k_w times the consumption time T_{con}. The outgassing length gives the upper limit of the depth of a mixed layer in which outgassing can compete with consumption as a sink for the trace species.

5. L_{comp} is the compensation depth. It represents the depth at which insolation can maintain a concentration in equilibrium with the atmosphere in the presence of consumption:

$$L_{\text{comp}} = \frac{P_{\text{con}} Q T_{\text{con}}}{[\text{CO}]_{\text{eq}}} \tag{10}$$

Examining (9) it can be seen that when D_{mix}/L is small

$$\frac{d}{dt}[\text{CO}] \sim P_{\text{con}} Q_0 / L - \text{other terms} \tag{11}$$

while when it is large

$$\frac{d}{dt}[\text{CO}] \sim P_{\text{con}} Q_0 / D_{\text{mix}} - \text{other terms} \tag{12}$$

Thus the ratio D_{mix}/L governs the importance of mixing in diluting the production.

D_{mix} also plays a role in determining which sinks of CO are most important. If the CO concentration is much larger than $[\text{CO}]_{\text{eq}}$ (as *Conrad et al.* [1982] argue is frequently the case) taking the ratio of the consumption sink term in (4) to the outgassing term gives

$$\frac{\text{consumption}}{\text{outgassing}} = \frac{D_{\text{mix}}}{k_w T_{\text{con}}} = \frac{D_{\text{mix}}}{L_{\text{out}}} \tag{13}$$

Thus the ratio $D_{\text{mix}}/L_{\text{out}}$ governs whether outgassing is more important than biological consumption.

Gas exchange can, however, be a source for CO as well as a sink. Suppose D_{mix} is larger than L. Then the ratio between the average production within the mixed layer $P_{\text{con}} Q_0 / \pi$ and the average consumption within a mixed layer at equilibrium with the atmosphere $D_{\text{mix}}[\text{CO}]_{\text{eq}}/T_{\text{con}}$ is just $D_{\text{mix}}/L_{\text{comp}}$. If $D_{\text{mix}}/L_{\text{comp}}$ is greater than 1, the atmosphere will tend to flux CO to the ocean. If $D_{\text{mix}}/L_{\text{comp}}$ is very small, then the solar production can easily keep up with outgassing and the ocean will flux CO to the atmosphere.

The depth of the permanent stratification or water depth H serves as an upper limit for D_{mix} and thus plays a role in setting a upper limit for $D_{\text{mix}}/L_{\text{out}}$ and D_{mix}/L. When D_{mix}/H is small increasing the strength of the mixing (either though increasing surface heat loss or wind stress) increases D_{mix}. When D_{mix}/H is of order 1, increasing the forcing has little or no effect on D_{mix}.

The remainder of this section presents nine dynamical regimes which are implied by four nondimensional numbers and considers what conditions might give rise to them. Figure 3a illustrates the "phase space" of the six regimes for which

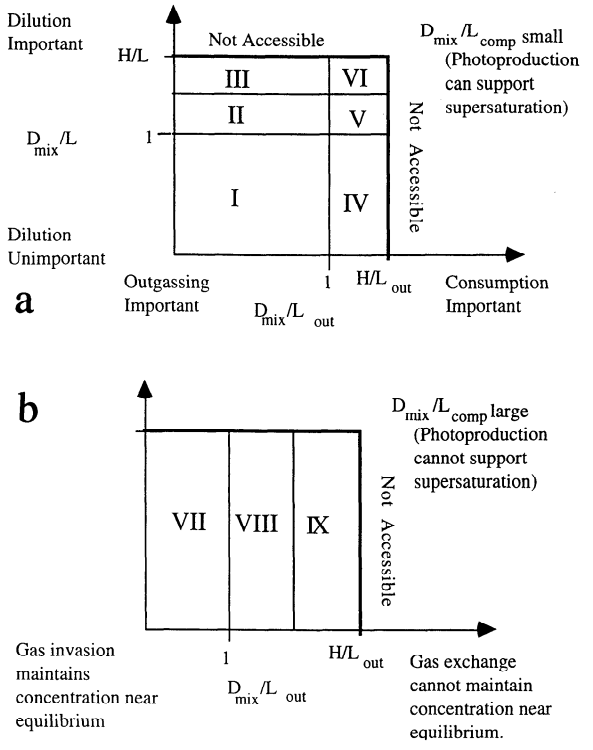

Figure 3. Phase diagram of the dynamics of a photochemical trace species as a function of ratios of the important length scales. D_{mix} is the mean mixed layer depth, H is the upper limit for that depth, set by the permanent stratification or the water depth, L_{out} is the outgassing length, L_{comp} is the compensation depth, and L is the e-folding scale of the photochemically active radiation. D_{mix}/L is a measure of the importance of dilution, D_{mix}/L_{out} a measure of the importance of outgassing versus biological consumption. D_{mix}/L_{comp} determines whether photochemical production can maintain a concentration greater than atmospheric equilibrium. (a) Assuming D_{mix}/L_{comp} small (production can produce supersaturation). Regime I, production not diluted; mixing across base of layer is a source; and outgassing primary sink. Regime II, production diluted by mixing; outgassing primary sink. Regime III, production diluted by mixing, but dilution limited by lower boundary; outgassing primary sink. Regime IV, production not diluted; consumption primary sink. Regime V, production diluted by mixing; consumption primary sink. Regime VI, production diluted by mixing, but dilution limited by lower boundary; consumption primary sink. (b) Assuming D_{mix}/L_{comp} large (production rarely or never produces supersaturation, gas exchange is the major source). Regime VII, gas exchange maintains concentration near equilibrium; very weak diurnal cycle. Regime VIII, gas exchange cannot always keep up with consumption; diurnal cycling with concentrations approaching equilibrium as layer shallows; increased wind produces both increased gas exchange and mixing. Regime VIX, gas exchange cannot keep up with mixing; weak diurnal cycling; increased wind stress produces higher levels of trace species.

D_{mix}/L_{comp} is small (production can maintain supersaturated mixed layer concentration) in terms of the ratios D_{mix}/L and D_{mix}/L_{out}. Figure 3b illustrates the phase space of three additional regimes when D_{mix}/L_{comp} is large (production is not capable of maintaining supersaturation within the mixed layer). It must be remembered that Figure 3 is a rough schematic. In reality the boundaries between the different regimes will have some width to them.

3.1. Regime I

$D_{mix}/L_{comp} < 1$, $D_{mix}/L < 1$, and $D_{mix}/L_{out} < 1$. In this regime, outgassing rather than consumption is the most important sink. An example of physical conditions which would give rise to such a dynamical regime given a small T_{con} would be a riverine plume or a very shallow layer created by rain. Given a larger value of T_{con}, this regime might occur in the open ocean on days when the insolation is very strong. Since $D_{mix} < L$, there will be production below the mixed layer and mixing across the mixed layer base can be an important source.

Regime I can exhibit counterintuitive behavior with regard to the dependence of the concentration and flux of CO on wind speed. As the wind speed increases, both the mixed layer depth and the transfer velocity increase. If the mixed layer depth increases faster than the gas exchange but $D_{mix}/L_{comp} < 1$, the concentration of CO at the surface can increase (essentially, the surface can draw on a larger pool of CO as a result of increasing mixed layer depth).

3.2. Regime II

$D_{mix}/L_{comp} < 1$, $H/L > D_{mix}/L > 1$, and $D_{mix}/L_{out} < 1$. In this regime, mixing is important both for diluting the production and limiting the effectiveness of outgassing in removing CO from the mixed layer. Within this regime,

$$[CO] \sim QF(D_{mix}/k_w)/D_{mix} \tag{14a}$$

$$F_{CO} \sim Qk_wF(D_{mix}/k_w)/D_{mix} \tag{14b}$$

and the model scalings are even more complicated functions of wind stress and heat flux. Most of the production occurs within the mixed layer, and mixing across the base is not as important. This regime corresponds to a scenario where the consumption time is very long (such as some of the observations north of Puerto Rico by *Jones and Amador* [1993]).

3.3. Regime III

$D_{mix}/L_{comp} < 1$, $H/L \sim D_{mix}/L > 1$, and $D_{mix}/L_{out} < 1$. In this dynamical regime the mixing is strong enough so that the lower boundary condition sets a limit on it. As in regime II, most of the production will occur within the mixed layer. A physical example of this scenario would be rather turbid coastal water on the shelf (for which L would be quite small) over which a very strong wind is blowing. For this case,

$$[CO] \sim QF(1/\tau^{1/2}) \tag{15}$$

so that increasing Q will increase the concentration while increasing τ will decrease the concentration.

3.4. Regime IV

$D_{mix}/L_{comp} < 1$, $D_{mix}/L < 1$, and $D_{mix}/L_{out} > 1$. In this regime the photochemical production is not substantially diluted by mixing and is largely balanced by biological consumption. The effects of mixing are negligible and

$$[CO] \sim Q \tag{16a}$$

$$F_{CO} \sim Q\tau^{1/2} \tag{16b}$$

A scenario which would yield a regime such as this would be a very sunny, calm day in the middle of an oceanic gyre during which a shallow diurnal mixed layer could form and persist.

3.5. Regime V

$D_{mix}/L_{comp} < 1$, $H/L > D_{mix}/L > 1$, and $D_{mix}/L_{out} > 1$. In this regime the production is diluted by mixing and is balanced by biological consumption. If D_{mix}/L_{comp} is small, the scaling for the concentration and flux will go as

$$[CO] \sim Q/D_{mix} \tag{17a}$$

$$F_{CO} \sim Q\tau^{1/2}/D_{mix} \tag{17b}$$

An example of physical conditions which would fall into this regime would be a very sunny but moderately windy day in the middle of an ocean gyre with a deep thermocline (a brisk winter day off Bermuda). Such a day will be studied in section 4. In this regime there is now a potential for nonlinear dependence of the concentration and flux on the wind stress and insolation. As Q increases, D_{mix} will decrease and the concentration will increase faster than Q, complicating simple attempts to estimate a production coefficient. The dependence of F_{CO} on τ will be slower than $\tau^{1/2}$, since increasing the wind stress will increase the mixed layer depth as well as the piston velocity.

3.6. Regime VI

$D_{mix}/L_{comp} < 1$, $H/L \sim D_{mix}/L > 1$, and $D_{mix}/L_{out} > 1$. This case corresponds to a very windy day in a central gyre so that the mixed layer goes right down to the main thermocline. The production is strongly diluted and balanced by consumption. Interestingly, the scalings for the concentration and the flux will be identical to those for regime IV.

3.7. Regime VII

$D_{mix}/L_{comp} > 1$ and $D_{mix}/L_{out} < 1$. In this regime, gas exchange rather than photochemical production is a major source term, and the mixed layer is shallow enough to be completely ventilated. An example of this regime would be an extremely cloudy but calm day in a region such as the wintertime northeast Pacific, where T_{con} could be very large but Q could be very small. In such circumstances, the CO concentration will be near $[CO]_{eq}$ most of the time, exhibiting a small diurnal range.

3.8. Regime VIII

$H/L_{out} > D_{mix}/L_{comp} > 1$ and $H/L_{out} > D_{mix}/L_{out} > 1$. In this regime the mixed layer is extremely deep, too deep for the gas exchange or the production to keep up. An example would parts of the Orinoco plume (where T_{con} is very small) during a storm. In such cases, the CO concentration will be smaller than $[CO]_{eq}$, and the gas exchange will serve as a primary source. The dependence of the CO concentration on wind stress is not obvious, since higher values of wind will produce more deepening (decreasing the CO concentration) as well as increasing the source strength.

3.9. Regime IX

$H/L_{out} \sim D_{mix}/L_{comp} > 1$ and $H/L_{out} \sim D_{mix}/L_{out} > 1$. In this regime the mixed layer penetrates all the way to the permanent stratification or the bottom, and the layer is so deep that it is not strongly ventilated within a consumption time. Examples might include Georges Bank during the wintertime or the Labrador Sea during episodes of deep convection. In such cases, increasing the wind speed will increase the CO concentration, by increasing the transfer of CO from atmosphere to ocean. The CO concentration will be quite low in such cases, quite a bit less than $[CO]_{eq}$.

Given a particular physical scenario which determines H, L, and T_{con}, not all of the regimes here will be accessible. If H is very small, and H/L is small (for example, in a very shallow, clear estuary), only regimes III and IV may be available. Given T_{con} extremely long, only regimes I, II, and III may be seen.

Rather than attempting to give examples of all of the dynamical regimes described here (for which complete data sets do not exist), a case representative of the interior of an oceanic gyre is examined below using the baseline KEA constants as defined above. These constants are used to force the mixed layer models through a 1-day cycle, to demonstrate the importance of dilution. Although dilution is shown to be important for this day, the agreement between models and data is far from perfect. The effect of forcing three different mixed layer models with a range of Q and τ is then presented so that the dependence of the dynamical regimes on the physical forcing, optics, and biology can be clarified. Last, the 1-day case is reexamined to see how varying the physics of the outgassing, the consumption rate, or production rate can result in a better fit to the data.

4. Model Results

4.1. Importance of Dilution and Sensitivity to Forcing

An example of the effect of dilution on the diurnal cycle of CO is shown in Figure 4, which shows contours of CO concentration in nM over the course of a day for four runs. Figure 4a shows the CO concentration contours for a case with no mixing, while Figures 4b–4d show the CO concentration for the MY2.5, PWP, and OPBL models, respectively. The day corresponds to that shown in Figure 1a, for which the mean wind stress was around 0.2 Pa (wind speed of 13 m s^{-1}), the peak insolation was around 800 W m^{-2} and the heat loss was 300 W m^{-2} [*Kettle*, 1994].

In the absence of mixing, there are strong vertical gradients in the concentration, with maximum surface concentrations of about 9 nM occurring approximately 9 hours after sunrise. These concentrations are much larger than those observed (by a factor of 6). In the presence of mixing, the concentration is homogenized over the top 40 m during the afternoon (6–12 hours after sunrise) and over the top 60–80 m during the following night (20–24 hours after sunrise) as nighttime heat loss results in mixed-layer deepening. The concentrations are much closer to the observed peak of about 1.5 nM. One can conclude then that mixing is potentially important in explaining the dynamics of CO in this case.

It is worthwhile to note some of the differences in model physics and how these influence the daily dynamics. The MY2.5 model has the least mixing of any of the three cases and predicts the largest values for surface CO concentration (~2.8 nM). The model develops a shallow (~20 m) mixed layer early in the day which then deepens steadily over the course of the day reaching a maximum depth of around 70 m the following morning. The PWP model also develops a shallow mixed in the early morning, but deepening occurs much more quickly. Indeed, several shallow layers develop and are mixed away over the course of the day. As a result more CO is exported from the euphotic zone than in the MY2.5 model and the peak surface concentrations are substantially smaller (2.3 nM). The OPBL model has a different behavior. During the morning, it retreats much more slowly than either the MY2.5 and PWP

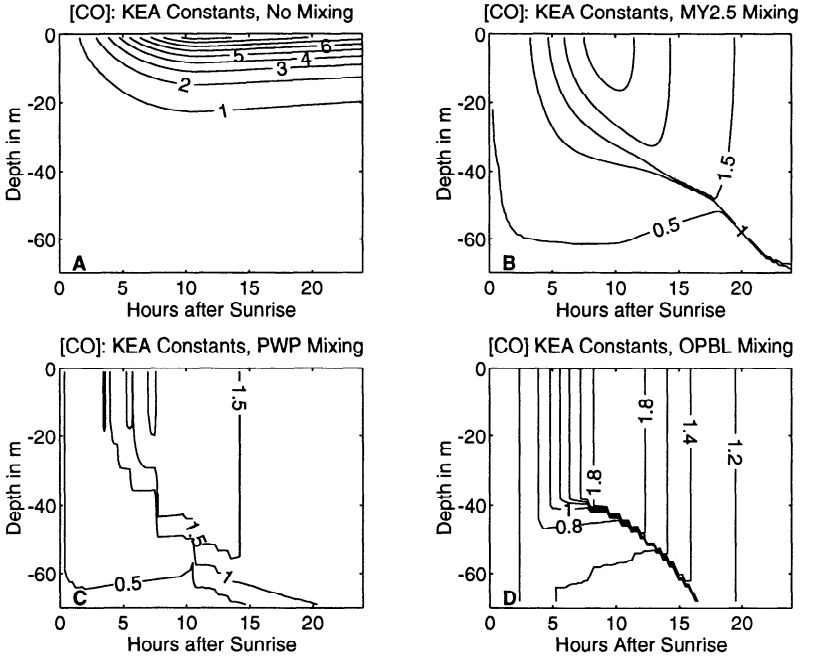

Figure 4. The effect of dilution on the diurnal cycle of carbon monoxide assuming the simplified production and consumption model presented in section 2 assuming a Jerlov water type of I. The peak insolation Q_i = 800 W/m^2 and the solar day is 12 hours long. The initial temperature profile is given by $T(z, t = 0) = 18 + 2.0*\tanh[(z - 87.5\text{ m})/7.5\text{ m}]$ so that there is an initial surface mixed layer with a temperature of 20°, a thermocline approximately 20 m thick centered around 87 m, and a deep ocean with a temperature of 16°. The e-folding scale of the shortwave (CO producing) radiation is taken to be 8 m, corresponding to the results of KEA. The wind stress is a constant 0.2 Pa. Conditions correspond to the day shown in Figure 1. (a) Contours of CO concentration in nM assuming no mixing. (b) Contours of CO concentration in nM assuming mixing given by the MY2.5 model. (c) Contours of CO concentration in nM assuming mixing given by the PWP model. (d) Contours of CO concentration in nM assuming mixing given by the OPBL model.

model, with minimum mixed layer depths of around 40 m being seen near noon. Thus more CO is mixed out of the euphotic zone and the peak surface concentrations are closer to the data (peak concentrations are ~1.95 nM). In the evening, the OPBL model deepens more quickly than the other two models.

In order to investigate the effect of heat flux, wind stress, and model parameterization on mixing, a series of runs is presented where the amplitude of the wind stress and the heat flux are varied. For convenience, the runs are chosen with the KEA model constants for production rate, consumption time, and $[CO]_{eq}$. For the first set of runs, a heat flux

$$Q(t) = Q_i(-\cos(2\pi t/T) - 1/\pi) \quad \cos(2\pi t/T) < 0 \qquad (18a)$$

$$Q = -Q_i/\pi \quad \cos(2\pi t/T) > 0 \qquad (18b)$$

is used which results in no net gain or loss of heat over the course of the day. Note that this means that the mixed layer will always mix down to the main thermocline at night, although the minimum mixed layer depth will depend on heat flux and wind stress. Q is varied from 100 W m^{-2} to 1000 W m^{-2} and the wind stress is varied from 0 to 0.45 Pa (corresponding to a windspeed of ~17 m s^{-1}). The models are integrated out over 30 days to reach a steady state. The results are indicative of the steady state toward which such a heat flux would tend to push the water column. Results in all cases are averaged over the final day of the integration. For these runs the main thermocline depth is taken to be about 55 m (shallower than the 85 m used for the runs in Figure 4 and more representative of the ocean in the mean).

Figure 5 shows contours of the mean surface concentration (left column), mean 20 m concentration (central column), and air-sea flux of CO (right column) as a function of wind stress and heat flux. The water type is taken to be Jerlov type I for which the e-folding scale of penetrating radiation is about 23 m, about 40% of the main thermocline depth H ~ 50–55 m. The compensation depth L_{comp} is around 400 m for Q = 1000 W m^{-2} and about 40 m for Q_i = 100 W m^{-2}.

The models exhibit broadly similar behavior for this particular forcing scenario. When the wind stress is very small and the heat flux is large (corresponding to regime IV), the mean concentrations at the surface are very large (up to 7 nM/L or 14 times the saturation level) for all three models. This is the right order of magnitude [*Conrad and Seiler*, 1986]. As τ becomes small there is essentially no mixing and the various models agree. The concentrations at the surface are a decreasing function of wind stress and an increasing function of the heat flux for all three models. This is especially true for low values of wind stress (0.1–0.2 Pa). At higher values of wind stress (corresponding to regime VI) the CO concentration is relatively insensitive to the actual value of wind stress. In all three models, the difference between the mean surface concentration for $\tau = 0$ and $\tau = 0.2$ Pa given the same insolation is of order 50%. This implies that dilution plays an important role in determining the surface CO concentration.

The behavior of the mean CO concentration at 20 m is also a strong function of wind stress and heat flux, but there are sometimes two separate wind stresses for which the concen-

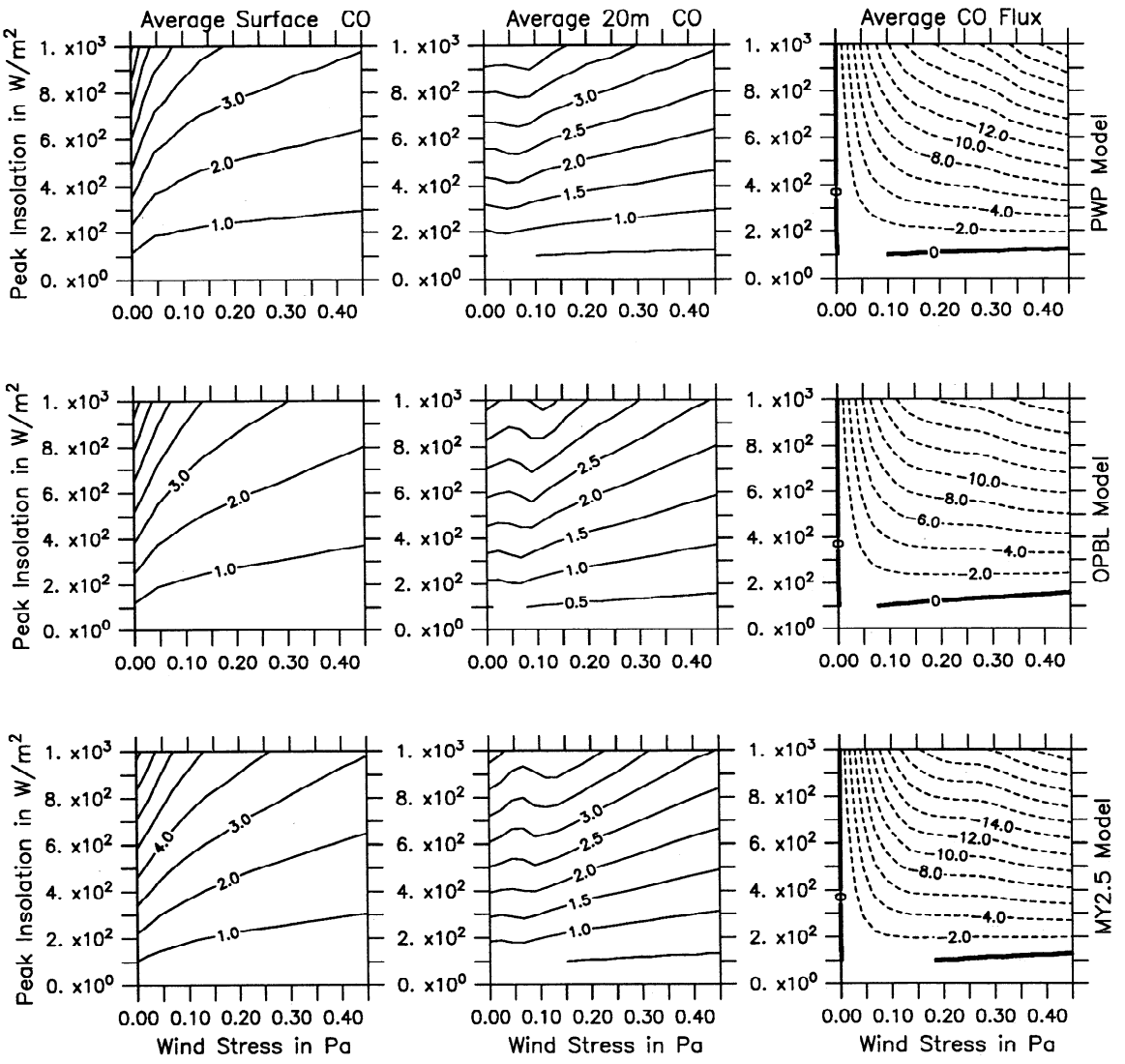

Figure 5. Dependence on the diurnal cycle of CO concentration on insolation, wind stress, and mixing parameterization. Vertical axis is peak insolation in W m^{-2}; horizontal axis is wind stress in Pa. Model runs are for KEA constants with the functional dependence of heating and wind stress and the initial temperature profile as in Figure 3 but with a thermocline at 50 m. (left) Daily-average surface CO in nM, (middle) column daily-averaged 20 m CO in nM, and (right) daily-averaged CO flux in μM m^{-2} d^{-1}. (top) PWP model, (middle) OPBL model, and (bottom) MY2.5 model.

tration is maximized (although the PWP model predicts only one). One maximum occurs when there is no mixing and biological consumption balances production, while the second maximum occurs because CO-rich surface water is mixed down to 20 m. Note that in the 30-day runs shown here, mixing occurs down to the main thermocline every night. For a single, sunny day during which the mixed layer experiences a net warming, the concentration at 20 m will exhibit even stronger variability as a function of wind stress. Similar results were found by *McNeil and Farmer* [1995] for oxygen produced by photosynthesis.

The right-hand column of Figure 5 shows the flux of CO in μmol m^{-2} d^{-1}. In a broad sense the gas flux is in an increasing function of heat flux and wind stress. However, it is interesting to note that for all the models there is a regime ($\tau > 0.2$ Pa, 600 W $m^{-2} > Q_i > 200$ W m^{-2}) where the dependence on wind stress is very weak. This is because as τ increases higher levels of dilution counteract the increase in piston velocity. Such a feature is predicted in section 3 to occur in regime V.

In general, outgassing is a sink for CO (fluxes are negative). However, for a few runs with low insolation and high winds, D_{mix} becomes larger than L_{comp}, and the atmosphere becomes a source, rather than a sink for CO. These cases fall onto the boundary between regimes V and VII and VI and VII, since most of the production occurs close to the surface and dilution is important. However, because of the long consumption time, gas exchange does have enough time to bring the concentrations back to near the equilibrium value of 0.5 nM.

4.2. Sensitivity to Model Constants: 30-Day Runs

The sensitivity of the concentration and flux to model constants and mixing parameterizations is now investigated by varying some of the constants from the standard ones used in the previous sections. The first constant of interest is the

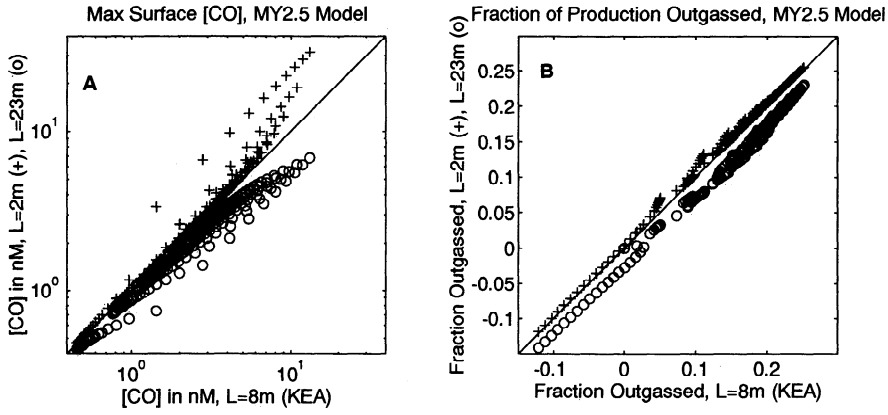

Figure 6. Dependence of flux and surface concentration on L, the e-folding scale of the photochemically active radiation. All runs shown are for the last day of a 30-day run of the MY2.5 model with 50-m mixed layer. (a) CO concentration: Horizontal axis is for L = 8 m, vertical axis is for L = 2 m (pluses) and 23 m (circles). Note that concentrations diverge for large values (D/L small) and converge at small values (strong mixing D/L large) (b) Fraction of production outgassed as a function of L. Note that dependence on L is much weaker for fraction outgassed than for mean concentration.

e-folding scale for the radiation L. Figure 6 shows the mean surface CO concentration and the fraction of the production outgassed (negative values mean gas exchange is a source) for the MY2.5 model (results are broadly similar for the other two models). Values for mean surface CO concentration and outgassing fraction are compared for L = 8 m (x axis) with L = 23 m (a value more in line with *Conrad and Seiler* [1986], who show considerable production at depths of 50 m) and L = 2 m (perhaps more appropriate for coastal waters). The surface concentrations are a strong function of L, particularly when the mixed layer is shallow and the concentrations are high. As the mixed layer becomes deeper (D_{mix}/L increases) and concentrations decrease as a result of dilution, the concentrations asymptote to a common value as predicted in sections 2 and 3. Note, however, that the order of magnitude differences seen in the surface CO concentration do not translate to order of magnitude differences in the flux, since they occur when the wind speed is low and thus the flux is small. The dependence of the flux on L alone is small for these cases which have large values of T_{con}. The fraction of CO outgassed is slightly larger for L = 2 m than for L = 8 m and slightly smaller for L = 23 m, but the differences are only of order 2% of the total production.

When variations in L are coupled to variations in the model physics, however, interesting differences begin to emerge. Figure 7 considers two chemical model parameter sets, the standard KEA values defined above, and another set with the same P_{con}, but with T_{con} = 12 hours, $[CO]_{eq}$ = 0.05 nM, and L = 2 m. This second parameter set is referred to as the Pristine Coastal parameter set and might be typical of a region where there is little pollution but considerable biological activity. There are systematic differences between the models and these differences are more pronounced when T_{con}, $[CO]_{eq}$, and L are small. The MY2.5 model predicts systematically higher values of surface concentration than the PWP model (up to 30% higher for the KEA constants, 50% higher with the Pristine Coastal constants), while the OPBL model predicts systematically lower values (as low as 30% lower). Differences between the OPBL and MY2.5 models can reach a factor of 2. These differences are reflected in the differences in fraction of CO outgassed, which is systematically lower for the OPBL and systematically higher for the MY2.5 model. Note that as T_{con} increases, it becomes increasingly difficult to drive large fluxes of the photochemically produced CO through the upper surface.

The differences between the models arise from the fundamental differences in the way in which mixing is parameterized. For the MY2.5 model, D_{mix} goes as $\sqrt{K_d T_{con}}$. If T_{con} = 12 hours, and K_d = 001–0.04 m^2 s^{-1} (roughly the range predicted for the day in question), D_{mix} is of order 20–40 m. Between the surface and D_{mix} there are gradients in CO concentration. In the PWP model, on the other hand, the mixed layer is completely homogenized. This means that the gradients predicted by the MY2.5 model are smoothed out so that the surface concentrations are smaller.

The OPBL model, on the other hand, predicts systematically deeper mixed layers than the PWP model and thus predicts even smaller surface concentrations. A principal reason for this is that the OPBL model allows buoyant convection to stir up dense water from below the mixed layer. Thus the PWP model predicts little entrainment from a diurnal cycle of heating with no net heat flux, while the OPBL model predicts that such a diurnal cycle will stir up fluid from the main thermocline. This sensitivity to heat loss also explains why the OPBL model shallows more slowly and deepens more quickly than the MY2.5 and PWP models for the 1-day case in Figure 4.

A parameter of interest to observers (as it is easily measured by continuous surface measurements such as those reported by *Conrad and Seiler* [1986]) is the timing of the maximum concentration. As noted earlier, in the absence of mixing, the timing of the maximum concentration can be used to infer the rate of biological consumption. As a general rule, the later in the day the maximum occurs, the smaller the biological consumption must be. If T_{con} = 52 hours as in the KEA parameter set, the maximum should occur near the end of the day, in the present case, approximately 12 hours after sunrise. For T_{con} = 6 hours (yielding a very fast consumption rate which may be characteristic of some coastal waters) the maximum should occur in the middle of the afternoon, or in the present case approximately 9 hours after sunrise. If T_{con} were very small (less than 1 hour), the maximum would occur at noon or 6 hours after sunrise in the present case.

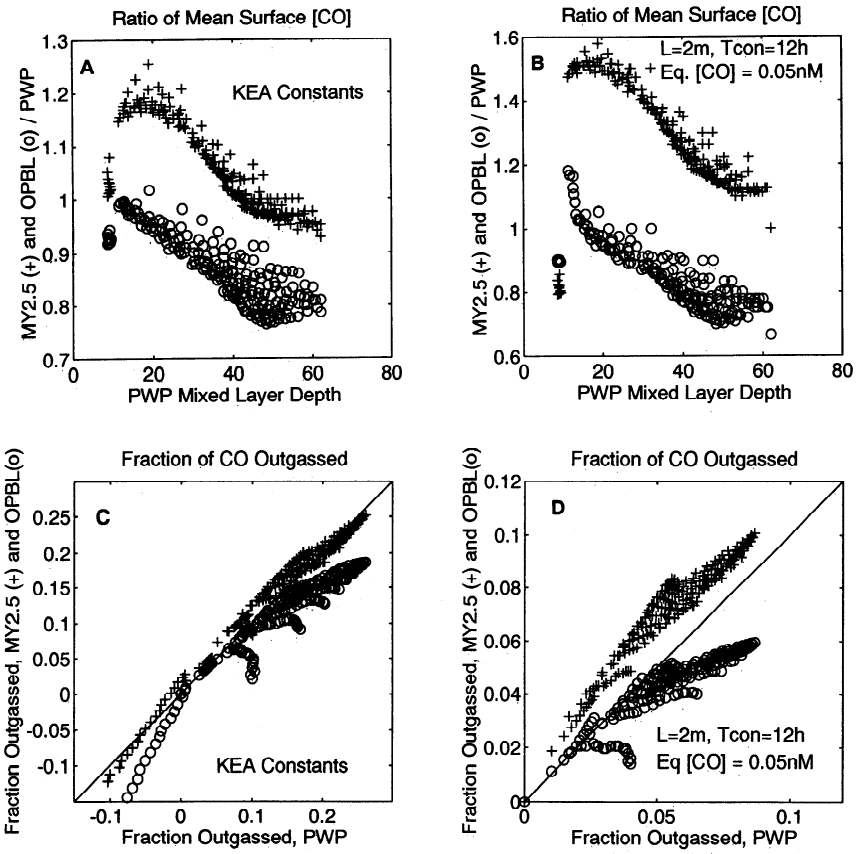

Figure 7. Dependence of CO concentration and outgassing fraction on parameterization of the mixing for two water types one described by the KEA constants (P_{con} = 14, T_{con} = 52 hours, L = 8 m $[CO]_{eq}$ = 0.5 nM), and the other by the Pristine Coastal constants (P_{con} = 14, T_{con} = 12 hours, L = 2 m $[CO]_{eq}$ = 0.05 nM). All results shown are for the last day of a 30-day integration. (a) Ratio of mean surface CO concentration predicted by MY2.5 (pluses) and OPBL (circles) models to that predicted by the PWP model. KEA constants. (b) Same as Figure 7a but for the Pristine Coastal constants. (c) Fraction of CO outgassed for the MY2.5 (pluses) and OPBL (circles) model versus fraction outgassed by the PWP model. Negative values mean gas exchange is a source. (d) Same as Figure 7c but for Pristine Coastal constants.

In the presence of mixing, the picture becomes more complex, as the maximum at depth can be shifted to later times (as CO-rich surface water is mixed downward), while the maximum at the surface moves earlier (to times before active mixing begins). Figures 8a and 8b demonstrate this fact for the maximum surface CO concentration using the MY2.5 model. When the diurnal mixed layer depth is small and T_{con} is large (Figure 8a), the maximum occurs late in the day. As the mixing increases, however, the time of the maximum shifts earlier in the day, eventually occurring at around 9 hours after sunrise. A similar, thought less marked pattern is seen for T_{con} = 6 hours (Figure 8b). Note, however, that in the presence of dilution, a sixfold decrease in consumption time produces less than a 1-hour change in the time of maximum surface CO concentration. When T_{con} = 52 hours, the pattern at depth (Figure 8c) is more marked, with the maximum for shallow diurnal mixed layers occurring ~18 hours after sunrise (around midnight).

It should be emphasized that the present case is somewhat artificial, in that the net heat flux over 1 day is not ususually zero, so that the mixed layer need not necessarily overturn once per day. When the mixed layer does not overturn within a consumption time (as in Figure 8d), a more complicated pattern develops. When the diurnal mixed layer is shallow, the maximum at depth occurs at roughly the same time as it does near the surface 8–9 hours after sunrise. As the mixed layer deepens, however, the time at which the maximum occurs increases to early in the evening (as the mixed layer passes through a 20-m depth bringing CO-rich surface water with it). Further mixing results in the CO-rich water being mixed to even greater depth, and the time at which the maximum occurs asymptotes around 8 hours after sunrise, the same as the surface. This result has important implications for estimation of P_{con} and T_{con} from surface or subsurface measurements. (A similar point is noted by *McNeil and Farmer* [1995] for oxygen.) On the one hand, in the presence of strong dilution, the maximum near-surface CO concentration will occur early in the day, leading to an underestimate of T_{con}. On the other hand, in the presence of weak dilution, the CO concentration maximum at some subsurface depth (say the intake depth of a ship) could occur later in the day as CO-rich surface water is mixed down, leading to a gross overestimate of T_{con}. This will be an especially severe problem in very turbid water in very calm conditions. In order to close the budget for CO it may prove necessary to measure at a number of points in the water column.

To summarize, the models all demonstrate that (1) the mean and peak CO concentration depend strongly on the wind stress; (2) when the mixing is weak, CO concentration also depends quite strongly on the water type; the flux, on the other

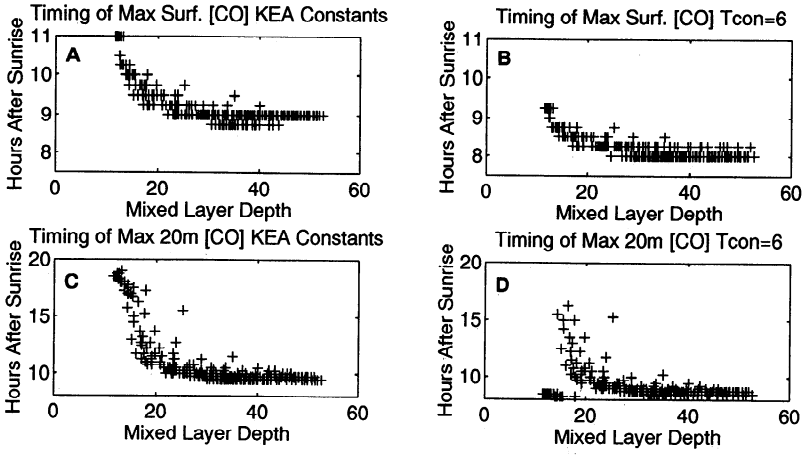

Figure 8. Dependence of the timing of the maximum concentration on mixed-layer depth and water type. All runs shown are for the MY2.5 model on the final day of a 30-day run. Horizontal axis is the daily-averaged mixed layer depth predicted by the MY2.5 model, vertical axis the number of hours after sunrise that maximum concentration occurs. (a) Time of maximum surface concentration, KEA constants. (b) Time of maximum surface concentration, KEA constants except that T_{con} = 6 hours. (c) Time of maximum concentration at 20 m depth, KEA constants. (d) Time of maximum concentration at 20 m depth, KEA constants except that T_{con} = 6 hours.

hand, is less sensitively dependent on L; (3) model parameterization can produce considerable differences in the surface CO concentration and flux of CO; these differences are most important when $H > D_{mix} > L$; and (4) the timing of the surface and subsurface maxima are strongly affected by dilution.

4.3. Modeling a 1-Day Time Series: Improving the Fit to the Data

The model runs presented in Figure 4 do not fit the data particularly well. The concentrations are all higher than observed, leading one to suspect some systematic error. This section will consider what sorts of modifications to the baseline chemical model might produce a better fit to the data. It will demonstrate, however, that fixes that produce agreement using one mixing model will not necessarily work with another.

The fact that the surface concentrations are too high leads one naturally to suspect that the production constant P_{con} is smaller than estimated by KEA. This is certainly a possibility, since the water on which the production estimates was made was collected during a different season from the data shown in Figure 1 and so might represent a different water type. Adjusting the production constant alone, however, does not fix all the problems. Figure 9 demonstrates this for the three models, reducing the production constant to fit the data. Note that the production constant needs to be reduced by 40% to provide a reasonable fit to the maximum for the PWP and OPBL models, but a reduction of 60% is called for to produce a fit to surface CO concentration in the MY2.5 model. Even with this reduction, however, the models do not reproduce the nocturnal decrease in CO concentration.

In order to produce lower nocturnal values of CO concentration it is necessary to provide a stronger sink. This is partially justifiable from data, since *Kettle* [1994] showed that consumption times over three incubations varied from ~20–100 hours. Figure 10 shows the effect of reducing T_{con} from 52 to 20 and 12 hours. Reducing the consumption time (and hence increasing the consumption rate) does produce more realistic nocturnal values. In fact, with a consumption time of 12 hours, the OPBL model does an excellent job at reproducing the data (a fact which will be returned to later). Notice, however, that reducing T_{con} still does not greatly improve the prediction of the morning values of CO concentration in either

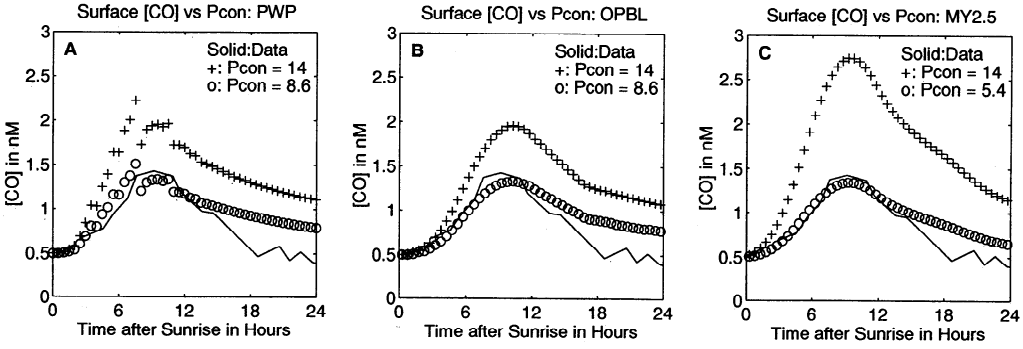

Figure 9. Bringing the model results in line with the data by changing P_{con}. Solid lines, the data from *Kettle* [1994]; pluses, KEA constants; and circles, with P_{con} reduced. (a) PWP model. (b) OPBL model. (c) MY2.5 model.

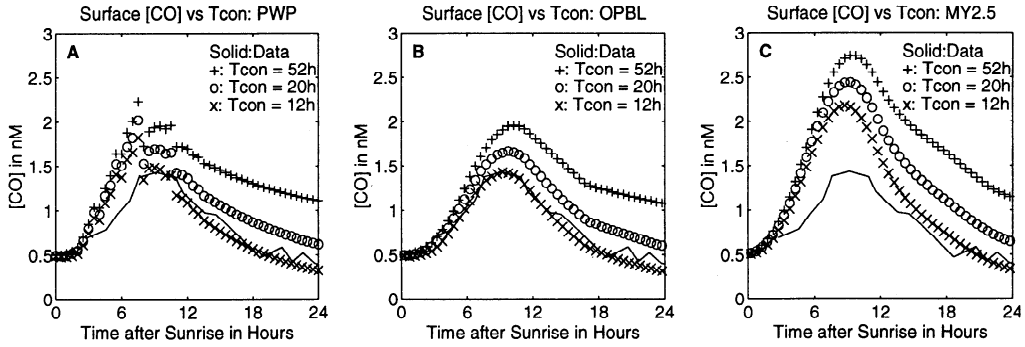

Figure 10. Bringing the model results in line with the data by changing T_{con}. Solid lines, the data from *Kettle* [1994]; pluses, the KEA constants (T_{con} = 52 h); circles, for T_{con} reduced to 20 hours (in line with the minimum from *Kettle* [1994]); and crosses, with T_{con} reduced to 12 hours. (a) PWP model. (b) OPBL model. (c) MY2.5 model.

the PWP or MY2.5 models, which are systematically too high. The PWP model, in particular, peaks far too early, and increasing T_{con} does nothing to help the problem. The essential problem may be that the PWP and MY2.5 models posit a quick retreat and slow deepening of the mixed layer, whereas the OPBL model posits a much slower retreat, requiring time for the turbulence within the layer to die out. This quick retreat (and subsequently small mixed layer depths during the early morning hours) is the main reason why the PWP and MY2.5 predict enhanced CO concentration at these times. The data seem more compatible with a slower increase, leading one to conclude that the OPBL model physics more accurately describes mixed layer dynamics on this day. This provides an example of how CO might be used to more accurately characterize the actual mixing physics of a mixed layer. In the absence of better agreement between the modeled concentrations given the measured constants and the data, however, it is premature to argue in favor of one mixing model over another.

An alternative hypothesis to the production or biological consumption being improperly modeled is that the gas exchange has been incorrectly specified. As noted by *Liss* [1984] chemical reactions at the interface can increase the rate at which gas is transferred. At low wind speeds, for example, carbon dioxide enters the water column more quickly than oxygen due to chemical interactions with the water. This hypothesis offers the additional attractions that it does not require any of the measured constants to be grossly in error and that it could offer a means of explaining subsurface maxima in

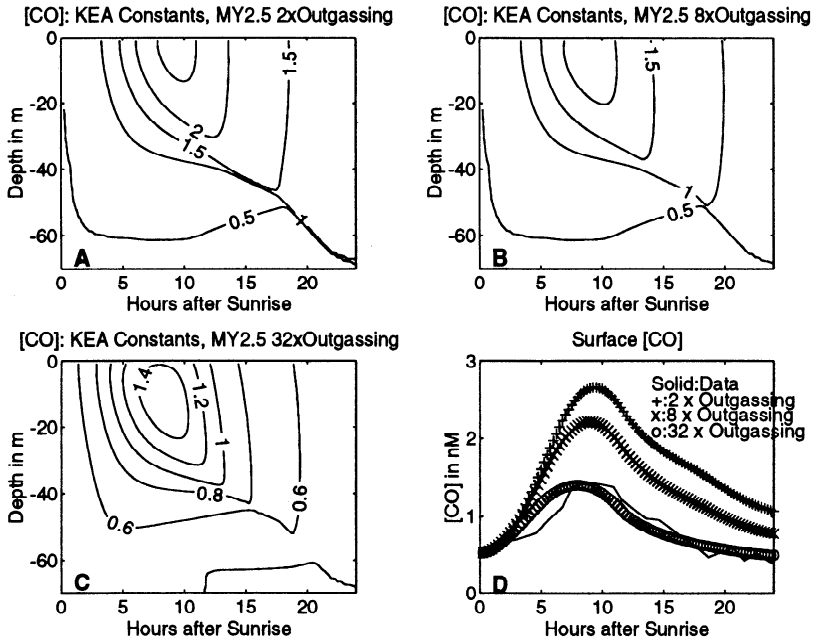

Figure 11. Bringing the model results in line with the data by increasing the strength of the outgassing. Model runs are identical to those in Figure 4 with different piston velocities. All runs are for MY2.5 model. (a) CO concentration for piston velocity 2X that estimated by *Liss and Merlivat* [1986]. (b) CO concentration for piston velocity 8X that estimated by *Liss and Merlivat* [1986]. (c) CO concentration for piston velocity 32X that estimated by *Liss and Merlivat* [1986]. (d) Surface concentrations for MY2.5 model and different values of piston velocity. Solid line, data; pluses, piston velocity twice Liss and Merlivat; crosses, piston velocity 8X Liss and Merlivat; circles, piston velocity 32X Liss and Merlivat.

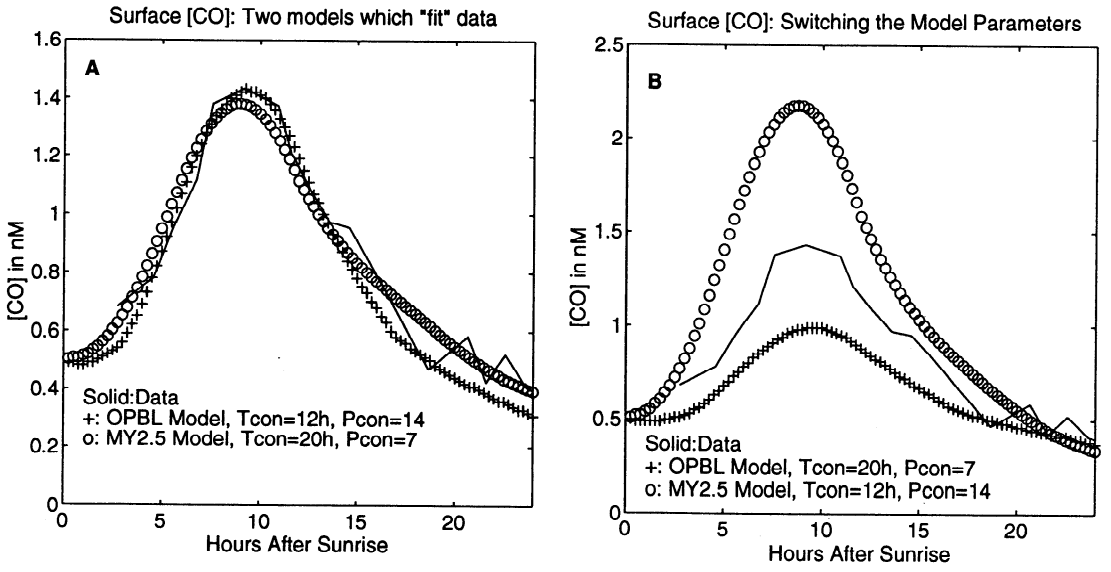

Figure 12. Sensitivity of surface CO concentration signal to model parameterization of mixing. (a) Two models which fit the data with different constants. Solid surface CO concentration in nM. Solid, data; pluses, OPBL model with P_{con} = 14 nmol W^{-1} h^{-1}; T_{con} = 12 hours, L = 8 m and outgassing given by *Liss and Merlivat* [1986]; circles, MY2.5 model with P_{con} = 7 nmol W^{-1} h^{-1}, T_{con} = 20 hours, L = 8 m and outgassing given by *Liss and Merlivat* [1986]. (b) Same models with constants switched.

CO concentration. However, as shown in Figure 11, the gas transfer equation needs to be in error by a considerable amount to reduce the surface concentrations to those observed and to produce a subsurface maximum in CO concentration. For a MY2.5 model, doubling the transfer velocity has little effect, and increasing it by a factor of 8 only reduces the excess surface concentration by 30%. The transfer velocity needs to be in error by a factor of 32 to reproduce the maximum surface CO concentration. Such large transfer velocities would be of geochemical interest since they would provide a mechanism for DOC to escape from the marine system, with upward of 80% of the CO escaping the ocean, in contrast to approximately 10% predicted for the Liss-Merlivat formulation. In the present case, however, increasing the transfer velocity, however, has the undesirable effect of shifting the time of the maximum concentration earlier in the day by about 2 hours than is actually observed. The model still fails to reproduce low morning concentrations.

A final illustration of the importance, not only of dilution but of its parameterization, is shown in Figure 12. The top panel shows that combinations P_{con} and T_{con} can be found so that different mixed layer models reproduce the observed surface concentrations. (The MY2.5 and OPBL models are chosen as the models which give the weakest and strongest mixing respectively, on this day, thus bracketing the uncertainty in the mixing.) Note, however, the differences in the necessary parameters. The MY2.5 model gives agreement with the data by producing half as much CO as the OPBL model and consuming it over twice the time. Thus different mixing models can produce a factor of 2 difference in the estimates for P_{con} and T_{con} when run in inverse mode. Note that when the model constants are switched (Figure 12b) the result is to accentuate the differences between the two models, which then differ by a factor of 3. This example clearly demonstrates the importance of correctly specifying the mixing.

5. Conclusions

The diurnal cycle of CO, and by extension a number of other chemical species, is strongly affected by the diurnal cycle of mixing. In section 2 it was argued that mixing would only be unimportant if the mean mixed layer depth D was much smaller than the e-folding scale of photochemically active radiation L and much larger than the outgassing length $L_{out} = k_w T_{con}$. Such a dynamical regime corresponds to a physical scenario with low wind, strong heating, and relatively fast biological consumption. In other cases, the concentration was predicted to depend on the wind stress as well as the insolation. The water type, which sets L, was shown to be important in determining the surface concentration. For a wide range of cases, dilution was shown to play an important role in setting both CO concentration throughout the water column and the flux of CO at the surface. For a wide range of cases it is necessary to correctly specify the mixing in order to reproduce the diurnal cycle. Models which parameterize mixing using eddy coefficients can give answers which are significantly different from models which parameterize the mixed layer as a homogeneous slab.

The results presented here are, of course, highly idealized. In the real world, the production and consumption are much more complicated than the model outlined here and may vary together. Nonetheless, it is encouraging that when reasonable values for the production and consumption constants are used, surface concentrations are obtained which are of the right order of magnitude in comparison to observations. Without a full set of measurements, which include more information about insolation, better estimates of production and consumption, and a detailed description of the actual evolution of the diurnal mixed layer it is wise not to push comparisons between models and data too far.

These results represent both a challenge and an opportunity

for observational oceanographers. They are challenging because they complicate the task of modeling certain photochemically produced compounds in the field. The fact that the diurnal cycle of CO depends on the mixing physics means that one needs to exercise care in using mixed layer models to estimate such important parameters as the production and consumption rates based on the surface concentration. Such problems may be avoided to some extent by taking frequent CTD profiles, so long as one is careful to look at the variation in the diurnal mixed layer rather than that of the main thermocline. The diurnal thermocline at the base of such mixed layers may have a very small temperature range (of order a few hundredths of a degree) requiring a high degree of precision. However, since much CO data are collected from ships which are underway, this is not a viable option much of the time. The results also demonstrate that the peak CO concentration at the surface is a strong function of water type. This is supports the use of more sophisticated optical models, such as those of *Sikorski and Zika* [1993a] and *Kettle* [1994] to capture the profile of the production in realistic oceanic cases, but only when the mixing is weak.

The results presented here represent an opportunity for observational oceanographers in that they offer a new window for examining the diurnal cycle of mixing. Traditionally, the diurnal cycle has been studied using the temperature signal over the course of the day. The problem with doing this is the presence of large, persistent features such as fronts or eddies whose associated temperature signals (1–2°C) are as large, if not larger than the diurnal variability. Chemical species such as carbon monoxide have the advantage of being "reset" by biological consumption each day. If it is possible to estimate the rate constants for production and consumption and if these constants are relatively homogeneous over the ocean interior (something which is still far from clear), it would be possible to use the diurnal cycle of photochemically produced species to distinguish between different mixed layer models. Note that during the day modeled in this study, the diurnal temperature excursion was extremely small (less than 0.05°C), but the surface CO concentration still varied by a factor of 3. Insofar as the production, consumption, and air-sea exchange of CO could be better quantified, CO might serve as a useful tracer on days when the mixing is strong. This is a promising possibility which deserves further study.

Acknowledgments. Thanks are due to Ollie Zafiriou for inspiring this work, Jim Price for lending me his model codes and for useful discussion, Roland Garwood for the OPBL model, Scott Doney for pointing out the importance of the main thermocline, and Jamie Kettle and Bill Martin for sharing their data. I thank the Office of Naval Research for supporting me as a Graduate Fellow. Final work on this manuscript was supported by the Office of Naval Research under grant N0014-90-J-1495. Contribution 8732 of the Woods Hole Oceanographic Institution.

References

Conrad, R., and W. Seiler, Photooxidative production and microbial consumption of carbon monoxide in seawater, *FEMS Microbiol. Lett.*, *9*, 61–64, 1980.

Conrad, R., and W. Seiler, Utilization of traces of carbon monoxide by acrobic oligotrophic microorganisms in ocean, lake, and soil, *Arch. Microbiol.*, *132*, 41–46, 1982.

Conrad, R., and W. Seiler, Exchange of CO and H_2 between ocean and atmosphere, in *The Role of Air-Sea Exchange in Geochemical Cycling*, edited by P. Buat-Menard, pp. 269–282, Kluwer, Norwell, Mass., 1986.

Conrad, R., W. Seiler, G. Bunse, and H. Giehl, Carbon monoxide in seawater (Atlantic Ocean), *J. Geophys. Res.*, *87*, 8839–8852, 1982.

Doney, S. C., R. M. Najjar, and S. E. Stewart, Photochemistry, mixing, and diurnal cycles in the upper ocean, *J. Mar. Res.*, *53*, 341–369, 1995.

Garwood, R. W., An oceanic mixed layer model capable of simulating cyclic states, *J. Phys. Oceanogr.*, *7*, 455–468, 1977.

Gnanadesikan, A., Dynamics of Langmuir circulation in the oceanic surface layer, Ph.D. thesis, 354 pp., MIT/WHOI Joint Program in Phys. Oceanogr., Woods Hole, Mass., 1994.

Gnanadesikan, A., and R. A. Weller, Structure and instability of the Ekman spiral in the presence of surface gravity waves, *J. Phys. Oceanogr.*, *25*, 3148–3171, 1995.

Jones, R. D., Carbon monoxide and methane distribution and consumption in the photic zone of the Sargasso Sea, *Deep Sea Res.*, *38*, 625–635, 1990.

Jones, R. D., and J. A. Amador, Methane and carbon monoxide production, oxidation, and turnover times in the Caribbean Sea as influenced by the Orinoco River, *J. Geophys. Res.*, *98*, 2353–2359, 1993.

Jones, R. D., and R. Y. Morita, Carbon monoxide oxidation by chemolithotropic ammonium oxidizers, *Can. J. Microbiol.*, *29*, 1545–1551, 1983.

Kantha, L., and C. A. Clayson, An improved mixed layer model for geophysical applications, *J. Geophys. Res.*, *99*, 25,235–25,266, 1994.

Kettle, A. J., A model of the temporal and spatial distribution of carbon monoxide in the mixed layer, M.S. thesis, MIT/WHOI Joint Program in Chem. Oceanogr., Woods Hole, Mass., 1994.

Large, W. G., J. C. McWilliams, and S. C. Doney, Oceanic vertical mixing: A review and a model with a nonlocal boundary layer parameterization, *Rev. Geophys.*, *32*, 363–403, 1994.

Liss, P. S., Gas transfer: Experiments and geochemical implications, in *Air-Sea Transfer of Gasses and Particles*, edited by P. S. Liss and W. G. N. Slinn, pp. 241–248, D. Reidel, Norwell, Mass., 1984.

Liss, P. S., and L. Merlivat, Air-sea gas exchange rates: Introduction and synthesis, in *The Role of Air-Sea Exchange in Geochemical Cycling*, edited by P. Buat-Menard, pp. 113–127, Kluwer, Norwell, Mass., 1986.

McNeil, C. L., and D. M. Farmer, Observations of the influence of diurnal convection on upper ocean dissolved gas measurements, *J. Mar. Res.*, *53*, 151–169, 1995.

Mellor, G. L., and T. Yamada, A hierarchy of turbulence closure models for planetary boundary layers, *J. Atmos. Sci.*, *31*, 1791–1806, 1974.

Mellor, G. L., and T. Yamada, Development ofc a turbulence closure model for geophysical fluid problems, *Rev. Geophys.*, *20*, 851–875, 1982.

Mopper, K., X. Zhou, R. J. Kieber, D. J. Kieber, P. J. Sikorski, and R. D. Jones, Photochemical degradation of dissolved organic carbon and its impact on the oceanic carbon cycle, *Nature*, *353*, 60–62, 1991.

Price, J. F., R. A. Weller, and R. Pinkel, Diurnal cycling: Observations and models of the upper ocean response to diurnal heating, cooling, and wind mixing, *J. Geophys. Res.*, *91*, 8411–8427, 1986.

Price, J. F., R. A. Weller, and R. R. Schudlich, Wind-driven ocean currents and Ekman transport, *Science*, *288*, 1534–1538, 1987.

Sikorski, R. J., and R. G. Zika, Modeling mixed layer photochemistry of H_2O_2: Optical and chemical modeling of production, *J. Geophys. Res.*, *98*, 2315–2328, 1993a.

Sikorski, R. J., and R. G. Zika, Modeling mixed layer photochemistry of H_2O_2: Physical and chemical modeling of distribution, *J. Geophys. Res.*, *98*, 2329–2340, 1993b.

Stramma, L., P. Cornillon, R. A. Weller, J. F. Price, and M. G. Briscoe, Large diurnal sea surface temperature variability: Satellite and in situ measurements, *J. Phys. Ocean.*, *16*, 827–837, 1986.

Swinnerton, J. W., R. A. Lamontagne, and C. H. Cheek, The ocean: A natural source of carbon monoxide, *Science*, *167*, 984–986, 1970.

Wannikhof, R., Relationship between wind stress and gas exchange over the ocean, *J. Geophys. Res.*, *97*, 7373–7382, 1992.

Watson, A. J., R. C. Upstill-Goddard, and P. S. Liss, Air-sea exchange in stormy seas measured by a dual-tracer technique, *Nature*, *349*, 145–147, 1991.

A. Gnanadesikan, Program in Atmospheric and Oceanic Sciences, Princeton University, Box CN710, Princeton, NJ 08544.

(Received May 26, 1995; revised January 9, 1996; accepted January 24, 1996.)